frontiers | Frontiers in Marine Science

TYPE Original Research
PUBLISHED 21 March 2023
DOI 10.3389/fmars.2023.1121866

Check for updates

OPEN ACCESS

EDITED BY
Lijuan Feng,
Zhejiang Ocean University, China

REVIEWED BY
Yongkai Tang,
Freshwater Fisheries Research Center (CAFS), China
Guoxing Nie,
Henan Normal University, China

*CORRESPONDENCE
Yongjiang Xu
xuyj@ysfri.ac.cn

SPECIALTY SECTION
This article was submitted to Marine Fisheries, Aquaculture and Living Resources, a section of the journal Frontiers in Marine Science

RECEIVED 12 December 2022
ACCEPTED 03 March 2023
PUBLISHED 21 March 2023

CITATION
Zhou H, Jiang Y, Xu Y, Cui A, Feng Y, Jin Z and Wang B (2023) Histological, microecological and transcriptomic physiological responses underlying hypoxia and reoxygenation adaptation in yellowtail kingfish (*Seriola lalandi*). *Front. Mar. Sci.* 10:1121866. doi: 10.3389/fmars.2023.1121866

COPYRIGHT
© 2023 Zhou, Jiang, Xu, Cui, Feng, Jin and Wang. This is an open-access article distributed under the terms of the Creative Commons Attribution License (CC BY). The use, distribution or reproduction in other forums is permitted, provided the original author(s) and the copyright owner(s) are credited and that the original publication in this journal is cited, in accordance with accepted academic practice. No use, distribution or reproduction is permitted which does not comply with these terms.

Histological, microecological and transcriptomic physiological responses underlying hypoxia and reoxygenation adaptation in yellowtail kingfish (*Seriola lalandi*)

Heting Zhou[1,2], Yan Jiang[1], Yongjiang Xu[1]*, Aijun Cui[1], Yuan Feng[1,2], Zhixin Jin[1] and Bin Wang[1]

[1]Joint Laboratory for Deep Blue Fishery Engineering of Pilot National Laboratory for Marine Science and Technology (Qingdao), Yellow Sea Fisheries Research Institute, Chinese Academy of Fishery Sciences, Qingdao, China, [2]National Demonstration Center for Experimental Fisheries Science Education, Shanghai Ocean University, Shanghai, China

Yellowtail kingfish has emerged as one of the most promising marine fishes for aquaculture in China because it is tasty, fast growing, and has high economic value. To investigate the tolerance and adaptability to hypoxia of farmed yellowtail kingfish, juveniles were exposed to hypoxia (3.0 ± 0.5 mg/L) for 5 days and then returned to normoxia (7.5 ± 0.5 mg/L) for another 5 days. Using tissue sections and high-throughput sequencing technology, we investigated the histological, microecological, transcriptomic, and physiological adaptation mechanisms of yellowtail kingfish. The results showed that hypoxia increased the gill lamellae length and spacing, which were reversible post-reoxygenation. At the genus level, the relative abundances of *Prevotella*, *Bacteroides*, *Roseburia*, and *Blautia* in the gastrointestinal tract increased under hypoxia and were maintained post-reoxygenation. The liver transcriptome revealed that, compared with normoxia group, the different expression genes (DEGs) were mainly enriched in Steroid biosynthesis and PPAR signaling pathways in hypoxia group. Compared with normoxia group, the DEGs were mainly enriched in Ribosome biogenesis in eukaryotes, Steroid biosynthesis, Fatty acid biosynthesis, and PPAR signaling pathways in reoxygenation group. Furthermore, compared with hypoxia group, the DEGs were mainly enriched in Ribosome biogenesis in eukaryotes and Ribosome pathways in reoxygenation group. In contrast to normoxia, of the key genes of the PPAR signaling pathway, *FABP4* was significantly downregulated, and *SCD-1* and *FATP* were significantly upregulated. These findings indicated reduced lipid deposition and increased lipid decomposition in liver under hypoxia. The genes including *PPARα*, *SCD-1*, *ANGPTL4*, and *FASN* were significantly upregulated in lipid metabolism-related pathways, which indicated that lipid metabolism activity was more vigorous during reoxygenation. In contrast to the hypoxia group, almost all of the genes involved in Ribosome biogenesis in eukaryotes and Ribosome pathways for protein processing were significantly upregulated during reoxygenation; this is probably related to the clearance of misfolded proteins and the folding of the

new proteins repairing there is damage to the body. The present results shed light on the possible synergetic function of lipid metabolism, protein repairment and synthesis, and gastrointestinal microbiota in resistance and homeostasis maintenance of yellowtail kingfish coping with hypoxic stress in aquaculture.

KEYWORDS

Seriola lalandi, hypoxia and reoxygenation, gastrointestinal microbiota, lipid metabolism, gill remodeling

1 Introduction

Dissolved oxygen is a crucial ecological component for the survival of aquatic species because it is necessary for maintaining various life processes. Currently, global climate change-related events, such as acidification and abrupt temperature changes, have exacerbated the formation of low-oxygen zones in the ocean, which causes potential stress and harm to organisms in natural marine environments (Li et al., 2015; Kroeker et al., 2020; Vedor et al., 2021; Helly and Levin, 2004). Under land-based greenhouse, pond, and deep-sea cage culture conditions, farmed fish frequently experience hypoxic stress caused by issues such as high density, human intervention, and abrupt climate changes; such stress can cause severe physiological damage and even death (Jiang et al., 2022; Xiao, 2015; Moreira et al., 2017). Therefore, studying the mechanisms of adaptation and tolerance to hypoxia can help us understand how farmed fish resist and adapt to hypoxic conditions and in turn support the development of practical regulation technologies for the fish farming industry. Such research can also provide useful information on how fish populations in natural marine environments are changing.

The dissolved oxygen level has a significant influence on the life activities of fish. It has been reported that hypoxia affected a wide range of biological functions of farmed fish, including behavior, organ morphology, and energy metabolism. For example, under hypoxic conditions, turbot (*Scophthatmus maximus*) drastically reduced their food intake (Pichavant et al., 2000), Atlantic cod (*Gadus morhua*) adjusted to the hypoxic stress by slowing down their swimming activity and speeding up their respiration (Petersen and Gamperl, 2010). The morphology of the gill reversibly changed in crucian carp (*Carassius carassius*) and blunt snout bream (*Megalobrama amblycephala*) when oxygen levels changed from hypoxic to normal oxygen levels (Sollid et al., 2003; Wu et al., 2017). These fish responded to hypoxic stress by increasing the surface area of the gill lamellae and the number of erythrocytes. Additionally, the secondary gill lamella swelled under hypoxic stress in golden pompano (*Trachinotus ovatus*) (Sun et al., 2021).

Fish have evolved different kinds of physiological mechanisms to cope with low oxygen over a long period of biological evolution. For example, short-term acute hypoxia triggers the activation of cellular pathways such as the HIF-mediated transcriptional activation response and the mTOR signaling pathway (Pawlus and Hu, 2013). When organisms encounter hypoxic conditions, they first activate complex cellular metabolic and physiological systems to maintain oxygen homeostasis (Dunwoodie, 2009). Furthermore, transcriptome analysis showed that the main energy supply pathway of large yellow croaker (*Larimichthys crocea*) was altered under hypoxic stress (Ding et al., 2020), and lipid metabolism was thought to be the main form of energy metabolism in golden pompano under hypoxic conditions (Sun et al., 2021). Effects of hypoxia on the intestinal microflora of juvenile cobia (*Rachycentron canadum*) showed that the richness and diversity of intestinal microflora significantly changed in response to hypoxic stress; additionally, the structure of the intestinal microbial population was altered (Wang et al., 2021). Some studies have proposed that gastrointestinal microbiota participate in the immune and metabolic processes by participating in some signaling pathways in vertebrates (Ramírez et al., 2020; Zhou et al., 2022). The interaction mechanism between gastrointestinal microorganisms and host gene regulation has provided a deeper insight into the adaptation mechanism of physiological changes in the organism in recent years (Ursell et al., 2014; de Vos et al., 2022). Although many studies have been carried out, the specific mechanisms underlying hypoxic stress adaptation of fish are still inadequately addressed.

Yellowtail kingfish is a pelagic species widely distributed in global oceans that spawns and grows naturally in the Yellow Sea and Bohai Sea of China. It is one of the best species for deep-sea cage and land-based greenhouse culture because of its powerful swimming ability, fast growth performance, high economic value, and high international consumption market demand (Liu et al., 2017; Xu et al., 2019; Li et al., 2022). Because of its rapid swimming and schooling characteristics, it is susceptible to hypoxia, which causes severe abnormal behaviors such as balance loss and frantic swimming. Thus, it is important to study the tolerance and adaptation ability of yellowtail kingfish to hypoxia, and the related mechanisms. The present study aimed to explore the tolerance and adaptation mechanisms of yellowtail kingfish juveniles under hypoxic stress and regeneration conditions based on histological, microecological, and transcriptomic analysis. The results could provide useful information on development of practical regulation technology for hypoxia adaptation of farmed yellowtail kingfish.

2 Materials and methods

2.1 Experimental design and sampling

The experimental fish were 6-month-old yellowtail kingfish in healthy condition, with an average body weight of 134.63 ± 10.06 g and body length of 19.82 ± 0.58 cm. Before the experiment, the fish were placed in white circular plastic tanks (400 L in volume) with sand-filtered sea water for 2 weeks to allow adaptation to a dissolved oxygen level of 7.5 ± 0.5 mg/L. The daily water change rate was 400% and the fish were fed a compound diet at 3% of their body weight once a day. The feeding was stopped the day before the start of experiment.

To determine the hypoxia level for this experiment, a pre-experiment was conducted. Twenty experimental fish were selected and placed in a white plastic circular tank (400 L in volume), the water in the tank was inflated with pure nitrogen to reduce the dissolved oxygen level. The suffocation point of dissolved oxygen for yellowtail kingfish juveniles was set at the level when the fish stopped swimming and rolled along the bottom. The pre-experiment revealed that, when the dissolved oxygen level was 2.56 mg/L, some of the experimental fish swam at the bottom of the water, and their swimming speed became very slow; some of the fish even stopped swimming. When the dissolved oxygen level was 2.11 mg/L, all the experimental fish stopped swimming, and some of the experimental fish lost balance and fell over after exposure to the dissolved oxygen level for 3 h. Thus, the asphyxiation point of yellowtail kingfish juveniles was judged to be 2.56–2.11 mg/L in pre-experiments. To ensure an accurate threshold of survival and adaptation of all experimental fish and reflect the actual hypoxia situation in the Yellow Sea and the Bohai Sea of China (Li et al, 2015; Shi, 2016), the dissolved oxygen level in experimental hypoxia group was maintained at 3.0 ± 0.5 mg/L.

The experimental containers were white circular plastic tanks (400 L in volume). A total of 120 experimental fish were arbitrarily selected and put into two experimental groups, the normoxia (DO) group and the hypoxia (LO) group; each group has three tanks, and 20 experimental fish were randomly put in each tank. After 5 days of hypoxic stress, the nitrogen inflation was stopped for the LO group and the dissolved oxygen level recovered to normoxia, which was then maintained for another 5 days; we named this the reoxygenation (RO) group. Dissolved oxygen levels were measured using an Orion fluorescence dissolved oxygen meter (USA, Thermo Fisher 120D-01A), and experimental water was sampled every 12 hours and the dissolved oxygen levels were validated in the laboratory according to the iodometric method of the international standard ISO 5813 1983. The dissolved oxygen levels during the experiment were monitored and are shown in Figure 1.

Nine experimental fish were taken from each group; that is, three fish were collected from each tank each time. The fish were anesthetized with MS-222 (10 mg/L), and the left third of gills were collected and preserved in Davis fixative for histological observation. Gastrointestinal tissues (stomach, pyloric caecum, intestine) and liver were dissected and placed in sterile, enzyme-free polypropylene centrifuge tubes; they were first preserved in liquid nitrogen and subsequently transferred to a −80°C freezer. The experimental procedure was approved by the Institutional Animal Care and Use Committee of Yellow Sea Fisheries Research Institute, Chinese Academy of Fishery Sciences.

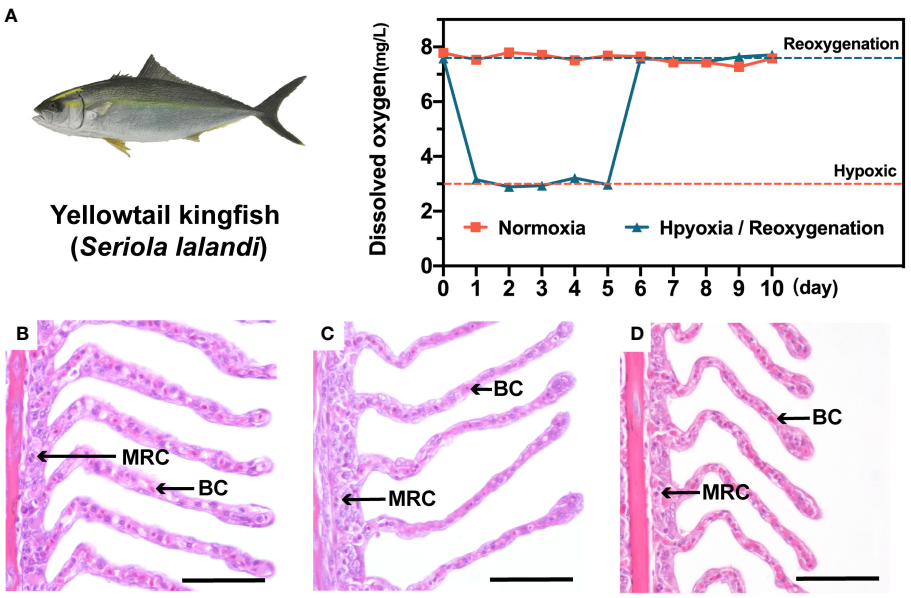

FIGURE 1
(A) Changes in dissolved oxygen levels in the experiment and corresponding gill tissue morphology. **(B)** is the normoxic level, **(C)** is the hypoxic level and **(D)** is the reoxygenation level. Scale bar: 50um. .

2.2 Histological changes in gills

Gill tissue was preserved in Davis fixative for 24 h, and then dehydrated and paraffin-embedded (55°C) and sectioned (5 μm). The section was stained with hematoxylin and eosin and photographed using a digital charge-coupled device camera (NIKON ECLIPSE 80i, NIKON DS-Ri1, Japan). The length, width, and interval of gill lamellae were measured using Image J 2020 software (NIH, USA).

2.3 Gastrointestinal microbiota sequencing

Genomic DNA was extracted from gastrointestinal tract samples using a DNA extraction kit (MagPure Soil DNA LQ Kit, Magen, China) following the manufacturer's instructions. The DNA concentration and quality were determined by spectrophotometer (NanoDrop 2000, USA) and 1% agarose gel electrophoresis. The genomic DNA was used as template for PCR amplification with barcoded primers and Tks Gflex DNA Polymerase (Takara, Japan). For the microbiota diversity analysis, the V3–V4 variable regions of the 16S rDNA gene were amplified using PCR with universal primers 343F (5′-TACGGRAGGCAGCAG-3′) and 798R (5′-AGGGTATCTAATCCT-3′) to amplify the 16S V3–V4 region.

Amplicon quality was visualized using gel electrophoresis, purified with AMPure XP beads (Agencourt, USA), and amplified for another round of PCR. After purification with the AMPure XP beads again, the final amplicon was quantified using a Qubit dsDNA assay kit. Equal amounts of purified amplicon were pooled for subsequent sequencing. The amplified sequences were detected by agarose gel electrophoresis for high-throughput sequencing using the Illumina MiSeq PE250 platform. The raw data obtained from sequencing were spliced and filtered with FLASH (version 1.2.11) (Magoč and Salzberg, 2011) and QIIME (version 1.8.0) (Caporaso et al., 2010) software to obtain valid data. Clean reads were subjected to primer sequence removal and clustering to generate operational taxonomic units (OTUs) using Vsearch software with 97% similarity cutoff. The representative read of each OTU was selected using the QIIME package. All representative reads were annotated and blasted against Silva database Version 138 using RDP classifier (confidence threshold of 70%).

2.4 Liver transcriptome sequencing

Total RNA was extracted from the liver samples of DO, LO, and RO groups using Trizol (Invitrogen, CA, USA). The extracted RNA was subjected to 1% agarose gel electrophoresis to detect the integrity of the total RNA. The concentration of RNA and the OD260/OD280 ratio were detected using a NanoDrop-2000 ultraviolet imaging system. Genomic DNA were removed using DNase I reagent (Takara). A TruSeq^{TM} RNA sample preparation kit (Illumina, San Diego, CA, USA) was used for RNA library construction. The mRNA was converted into stable double-stranded cDNA using the SuperScript double-stranded cDNA synthesis kit (Invitrogen, CA, USA) with a six-base random primer (Illumina). The product of the adaptor ligation was purified and fragments sorted, and PCR amplified the sorted product to obtain the purified library. Then, 200–300-bp bands from different groups were enriched and recovered using 2% agarose gel. The enriched cDNA was quantified using TBS380 (Picogreen) to obtain different cDNA libraries. The different cDNA libraries were high-throughput sequenced using the Illumina NovaSeq 6000 platform with a sequencing read length of PE 150 (Ma et al., 2022). FASTQ software was used to filter the raw data to ensure the data's reliability (Chen et al, 2018). Clean reads were produced by eliminating adapter- and poly-N-containing reads and low-quality reads from the original data.

The filtered clean reads were compared to the reference genome using HisAT2 software, and the positional information of clean reads on the reference genome was swiftly and precisely compared with the reference genome (https://www.ncbi.nlm.nih.gov/nuccore/JAIQDC000000000.1). The transcripts per million reads method was used to identify the expression level of each gene to identify differentially expressed genes (DEGs). Differential expression analysis was then performed using DESeq2 software (Love et al, 2014). To calculate gene abundance degree, RSEM was utilized (Li and Dewey, 2011). Significant DEGs were defined as those with $|\log2(\text{foldchange})| \geq 1$ and $P\text{-adjust} \leq 0.05$. Furthermore, Gene Ontology (GO) and Kyoto Encyclopedia of Genes and Genomes (KEGG) analyses were carried out to determine the functions and pathways associated with DEGs (San et al., 2021). GO functional enrichment and KEGG pathway analysis were carried out by Goatools (https://github.com/tanghaibao/Goatools) and KOBAS (http://kobas.cbi.pku.edu.cn/home.do) (Xie et al, 2011), respectively.

2.5 Data validation by quantitative analysis

Five DEGs involved in Steroid biosynthesis, PPAR signaling pathway, and Fatty acid biosynthesis were selected for quantitative real-time PCR (qRT-PCR) to determine the accuracy of the RNA-Seq data. The primers were designed using Primer Premier 5 software (Premier Biosoft International, United States) (Table 1). qRT-PCR was performed using a Roche Light Cycler 480II® (Roche). The qRT-PCR system was 10 μL and the amplification conditions were: 95°C for 30 s; 40 cycles at 95°C for 30 s and 60°C for 30 s. The *arp* gene was selected as the reference gene, and the $2^{-\Delta\Delta Ct}$ method was applied to determine the relative expression levels of target genes.

2.6 Statistical analysis

IBM SPSS 26 software was used for statistical analysis. Significant differences between samples were carried out by one-way analysis of variance (ANOVA) and Duncan's tests. The significance level was set at $P < 0.05$ and the experimental results are expressed as the mean ± standard deviation (SD).

TABLE 1 Primers used to validate the analysis of selected DEGs.

Primer name	Sequence (5′-3′)	Amplification target
FABP4	F: 5′GCGTGGGTGATGCTGGGGTTA3′ R: 5′CCGTCTGCGGTCGTCTCGTC 3′	qRT-PCR
FASN	F: 5′GAGCAGCAGCCAGCAGGGAC3′ R: 5′CGGGGACCGACAGCGACAA3′	qRT-PCR
FDFT1	F: 5′GAAACCTCGCTCAGGAATAC3′ R: 5′ATACTGGTCCCACTCCTTCA 3′	qRT-PCR
PPARα	F: 5′AGACCAGCACCCCTCCTTT3′ R: 5′CCTGTCCTTCAGCACTCCC 3′	qRT-PCR
SCD-1	F: 5′CATCCCTTCAGCATCTCCT3′ R: 5′AGTGGTAATGACGCCTTGT 3′	qRT-PCR
arp	F: 5′TGCCATTGTCATACACTTGCTG3′ R: 5′GGGGAACCATTGAAATCTTGAG3′	qRT-PCR

3 Results

3.1 Changes in gill structure in response to hypoxia

After 5 days of hypoxia, the number of blood cells (BC) and mitochondria-rich cells (MRC) in the gills were significantly higher in the LO group ($P < 0.05$). At the same time, the length of secondary gill lamellae and space between secondary gill lamellae showed a significant increase and the width of secondary gill lamellae decreased ($P < 0.05$) (Table 2, Figures 1B, C). In the RO group, these morphometric changes in gills recovered (Table 2, Figure 1D).

3.2 Microbiota analysis of the gastrointestinal tract

The results of 16S rRNA analysis of the microbiota in the stomach, pyloric caecum, and intestine of yellowtail kingfish are shown in Table 3. The Good's coverage of each sample was close to 1, which indicated that the sequencing data were suitable for subsequent microbial community structure analysis. The alpha diversity index showed that the chao1 index decreased in the gastric and pyloric caecum and increased in the intestine in the LO group, but the opposite trend was observed in the RO group. A comprehensive comparison of the OTUs of the microbiota throughout the entire gastrointestinal tract (stomach, pyloric caecum, intestine) (Figure 2A) revealed that their quantities changed under different oxygen conditions, but the composition of dominant microbiota remained stable.

At the phylum level (Figure 2B), the abundances of Bacteroidota and Firmicutes showed similar increasing trends in the LO and RO groups. However, the F/B ratio of Firmicutes and Bacteroidota was highest in the LO group, and the ratio in the RO and DO groups was similar. At the genus level (Figure 2C), the abundance of *Prevotella* increased in the LO group and continued to increase in the RO group. Moreover, the abundances of *Bacteroides*, *Roseburia*, and *Blautia* increased in that LO group and maintained high levels in the RO group. On the contrary, the abundance of *Faecalibacterium* decreased in the LO group, but increased in the RO group, but both were higher than in the DO group. These increased dominant bacteria all have the function of producing short-chain fatty acids (SCFA) among gastrointestinal microbiota.

According to KEGG analysis (Figure 3), the LO and RO groups clustered close to each other, and the DO group clustered far away from them. The clustering results of the LO and RO groups were similar, and they were mainly enriched in Glycan biosynthesis and metabolism and Signaling molecules and interaction.

3.3 Liver transcriptome analysis

A total of 504,542,314 raw sequencing reads and 500,468,058 clean reads after quality control filtering were obtained, and the clean data of each sample reached more than 7.51 Gb (Supplementary

TABLE 2 Indices of gill tissue after 5 days of hypoxia and 5 days of reoxygenation.

Group	numbers of BC	numbers of MRC	Length of secondary gill lamella(μm)	Width of secondary gill lamella(μm)	Space between secondary gill lamella(μm)
DO	25.22 ± 2.82^{a}	27.89 ± 2.15^{a}	135.91 ± 7.04^{a}	7.67 ± 1.37^{b}	23.29 ± 2.82a
LO	28.44 ± 2.46^{b}	31 ± 2.55^{b}	168.25 ± 8.18^{b}	6.29 ± 0.88^{a}	27.01 ± 2.48b
RO	24.11 ± 3.01^{a}	28.78 ± 2.64^{ab}	137.43 ± 8.17^{a}	7.73 ± 1.59^{b}	23.51 ± 2.74a

Different lowercase letters in the same column indicate significant differences, P<0.05.

10.3389/fmars.2023.1121866

TABLE 3 Gastrointestinal flora sequencing quality and alpha diversity.

Samples	Goods coverage(%)	chao1	Shannon	simpson
DOS	99.69 ± 0.01	1120.54 ± 32.22	6.65 ± 0.07	0.96 ± 0.01
DOP	99.7 ± 0.02	1214.47 ± 43.48	6.66 ± 0.59	0.95 ± 0.04
DOG	99.72 ± 0.01	980.13 ± 25.06	6.87 ± 0.13	0.97 ± 0
LOS	99.72 ± 0.02	1050.15 ± 63.82	7.34 ± 0.32	0.99 ± 0
LOP	99.75 ± 0.02	1009.74 ± 9.8	7.32 ± 0.02	0.99 ± 0
LOG	99.63 ± 0.02	1213.56 ± 65.12	7.22 ± 0.19	0.98 ± 0
ROS	99.62 ± 0.02	1241.78 ± 26.81	7.29 ± 0.09	0.99 ± 0
ROP	99.65 ± 0.03	1190.06 ± 48.99	7.23 ± 0.06	0.98 ± 0
ROG	99.67 ± 0.02	1103.14 ± 24.86	7.07 ± 0.34	0.98 ± 0.02

DOS, DOP, and DOG are the stomach, pyloric caecum, and intestine of the DO group, respectively, LOS and ROS, etc. are the gastrointestinal samples of the LO and RO groups.

Table 1). The percentage of Q30 bases was above 93.76% and the GC ratio was between 48.45%–50.86%, and over 95% of reads could be mapped to the yellowtail kingfish genome, which indicated that the sequencing data quality was sufficient to fulfill the requirements of the subsequent analysis. The principal component analysis plot of sequencing data revealed that samples in the same group were closely related but the groups were clearly separated (Figure 4A). Comparison between DO and LO groups produced 210 DEGs (Figure 4B), of which 107 were upregulated genes (URGs) and 103 downregulated genes (DRGs). Comparison between DO and RO groups produced 805 DEGs, of which 484 URGs and 321 DRGs were screened (Figure 4C). Comparison between LO and RO groups produced 1127 DEGs, of which 703 URGs and 424 DRGs were screened (Figure 4D).

The DEGs were annotated in the GO database, and the results showed that they were mainly involved in biological processes including cellular and metabolic processes (Figure 5). KEGG analysis indicated that URGs were significantly enriched in Steroid biosynthesis, and DRGs were significantly enriched in the PI3K-Akt signaling pathway and PPAR signaling pathway; however, most URGs and DRGs were simultaneously enriched in the Steroid biosynthesis and PPAR signaling pathways in the LO group (Figure 6A). In the RO group, URGs were significantly enriched in Ribosome biogenesis in eukaryotes, and DRGs were significantly enriched in the ECM-receptor interaction, and Ribosome biogenesis in eukaryotes, Steroid biosynthesis, Fatty acid biosynthesis, and PPAR signaling pathways were the major pathways that were simultaneously enriched in both URGs and

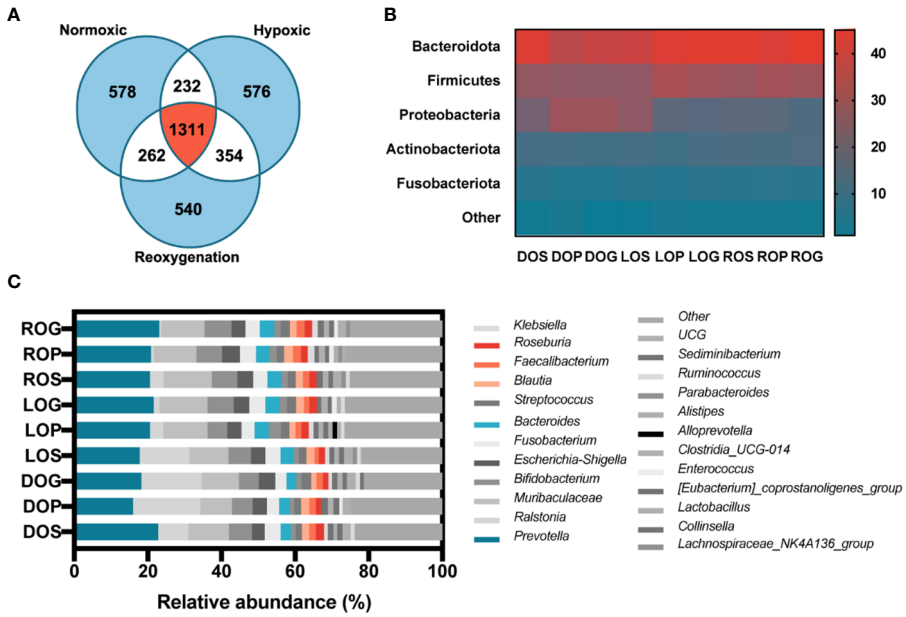

FIGURE 2
Gastrointestinal microbial structure **(A)** Venn diagram of the number of OUTs between different groups **(B)** Heat map of relative abundance at the phylum level **(C)** Structure of relative abundance at the genus level. DOS, DOP, and DOG are the stomach, pyloric caecum, and intestine of the normoxic group, respectively, LOS and ROS, etc. are the gastrointestinal samples of the hypoxic and reoxygenated groups.

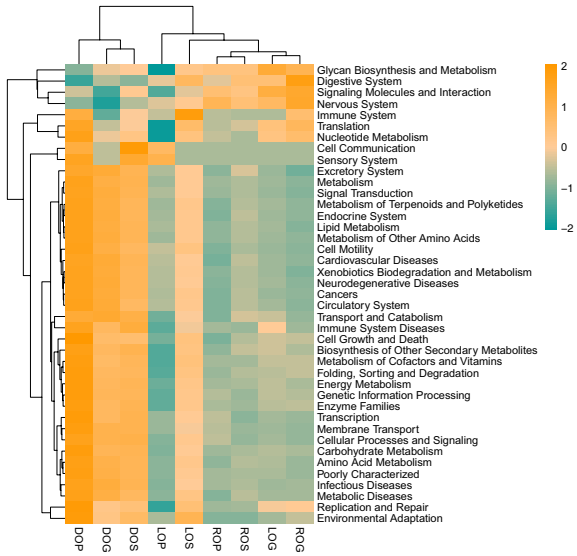

FIGURE 3
The functional clustering heatmap of microbiota was predicted based on KEGG database.

DRGs (Figure 6B). Comparison of the LO group and RO group showed that DEGs were mainly enriched in Ribosome biogenesis in eukaryotes and Ribosome function pathways (Figure 6C). In conclusion, most DEGs in liver were enriched in pathways related to energy metabolism, and protein synthesis during adaptation to hypoxia and reoxygenation conditions.

3.4 Validation of expression pattern of DEGs

The qRT-PCR amplification of the five selected genes showed the same expression patterns as the RNA-Seq results, which verified the specificity and accuracy of transcriptome expression analysis (Figure 7).

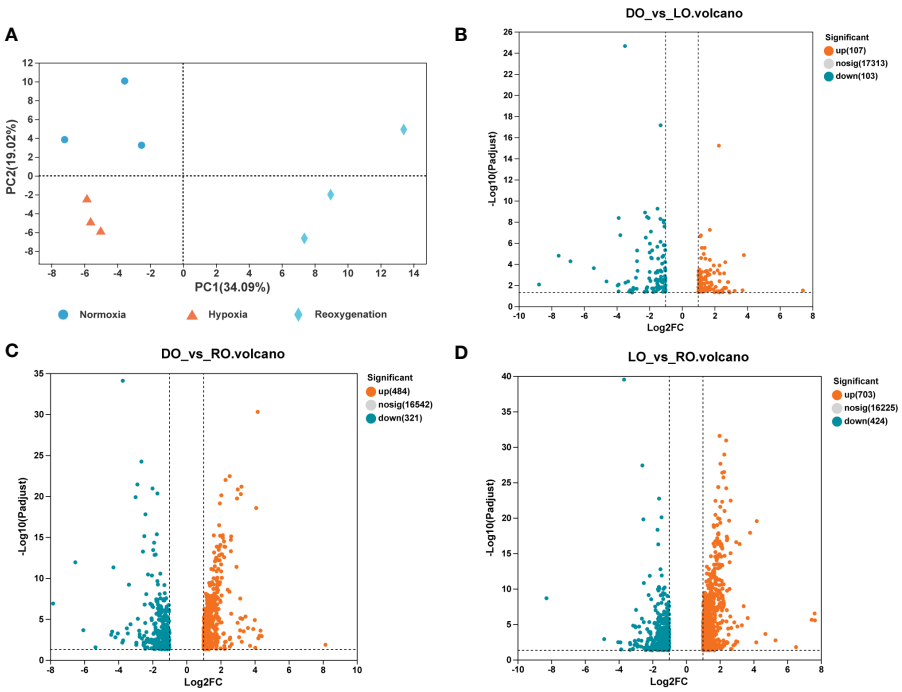

FIGURE 4
Clustering of liver samples and differentially expressed genes. **(A)** Two-dimensional principal component analysis (PCA) plots of liver transcriptome data **(B)** Map of DEGs volcanoes (normoxia vs hypoxia). **(C)** Map of DEGs volcanoes (normoxia vs reoxygenation). **(D)** Map of DEGs volcanoes (hypoxia vs reoxygenation).

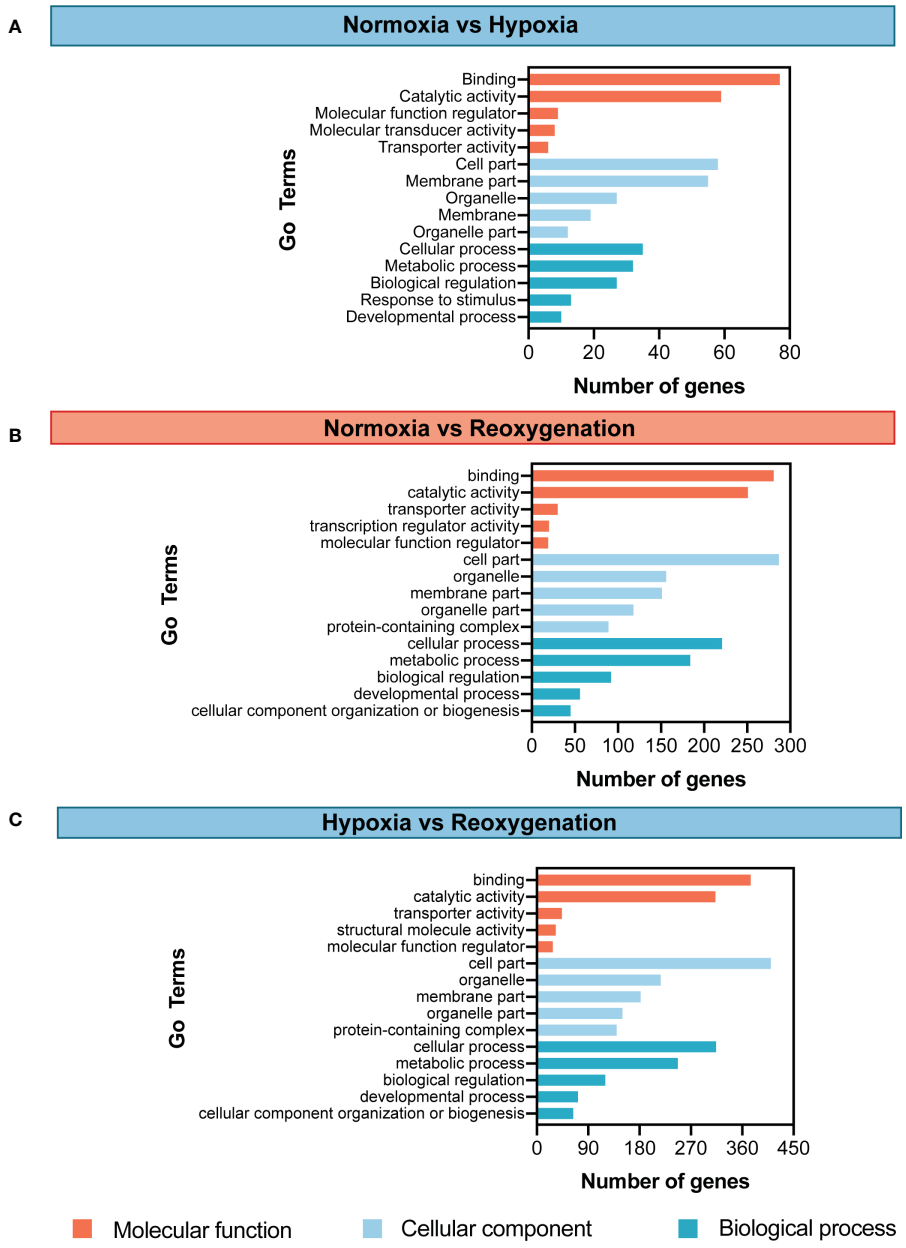

FIGURE 5
Annotation of differentially expressed genes. **(A)** GO annotation diagram for DEGs (normoxia vs hypoxia). **(B)** GO annotation diagram for DEGs (normoxia vs reoxygenation). **(C)** GO annotation diagram for DEGs (hypoxia vs reoxygenation).

4 Discussion

4.1 Adaptive changes in gill tissue structure during hypoxia and reoxygenation

To deal with hypoxic environments, fishes exhibit several morphological, physiological, and molecular responses to maintain homeostasis and organism functions. The fish gill is the dominant organ responsible for physiological exchanges with the surrounding environment, playing a primary role in gas exchange, and it is the first target under hypoxia (Evans et al., 2005). The physiological adaptation of fish to hypoxia results in an increase in the number of red blood cells, which are responsible for oxygen transportation (Xiao, 2015; Chen et al., 2017). It has been reported that golden pompano and blunt snout bream survive hypoxia by increasing the surface area in contact with oxygen by widening the spacing between gill lamellae, while the number of blood cells and the mitochondria-rich cells at the base of the gill lamellae significantly increase; these changes improve their ability to transport oxygen enhanced (Chen et al., 2017; Wu et al., 2017).

In the present study, the number of red blood cells and mitochondria-rich cells in the gill lamellae significantly increased in the LO group, the spacing and length of the gill lamellae significantly increased, and the width of the gill lamellae significantly decreased. After recovery for 5 days, the gill structure and the number of blood cells and mitochondria-rich cells showed

no significant difference compared with the DO group. These results suggested that yellowtail kingfish changed gill structure and cell quantities in response to hypoxic stress, and this course could be reversible after reoxygenation.

4.2 Association analysis between DEGs and microbiota based on KEGG enrichment

In present study, KEGG enrichment analysis indicated that, compared with the NO group, OTUs of microbiota from the LO group and RO group were mainly annotated to three major functions: Metabolism, Cellular Processes and Signaling, and Organizational system. Further analysis showed that pathways, including Glycan biosynthesis and metabolism, Digestive system, Signaling molecules and interaction, and Nervous system, are all related to energy

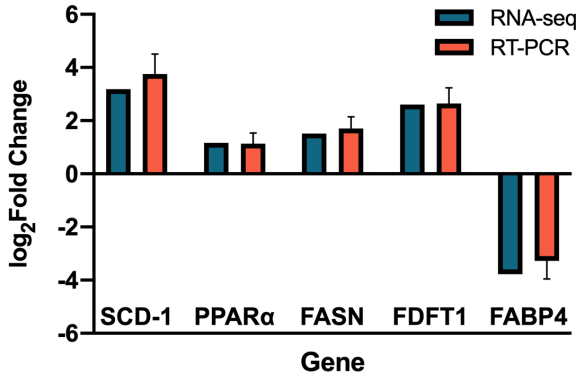

FIGURE 7
Comparison of gene expression data between RNA-seq and quantitative real-time PCR (RT-PCR).

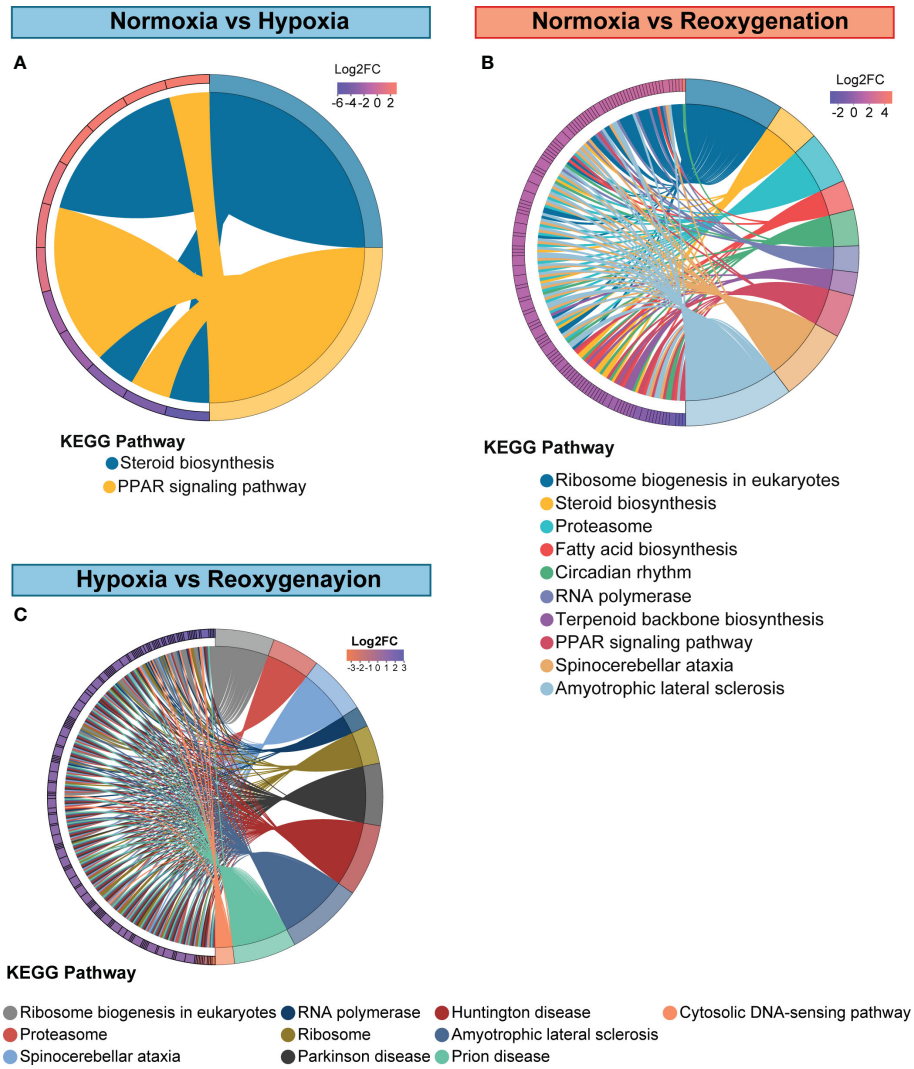

FIGURE 6
Pathway enrichment of differentially expressed genes. **(A)** KEGG chord plot diagram of DEGs (normoxia vs hypoxia). **(B)** KEGG chord plot diagram of DEGs (normoxia vs reoxygenation). **(C)** KEGG chord plot diagram of DEGs (hypoxia vs reoxygenation).

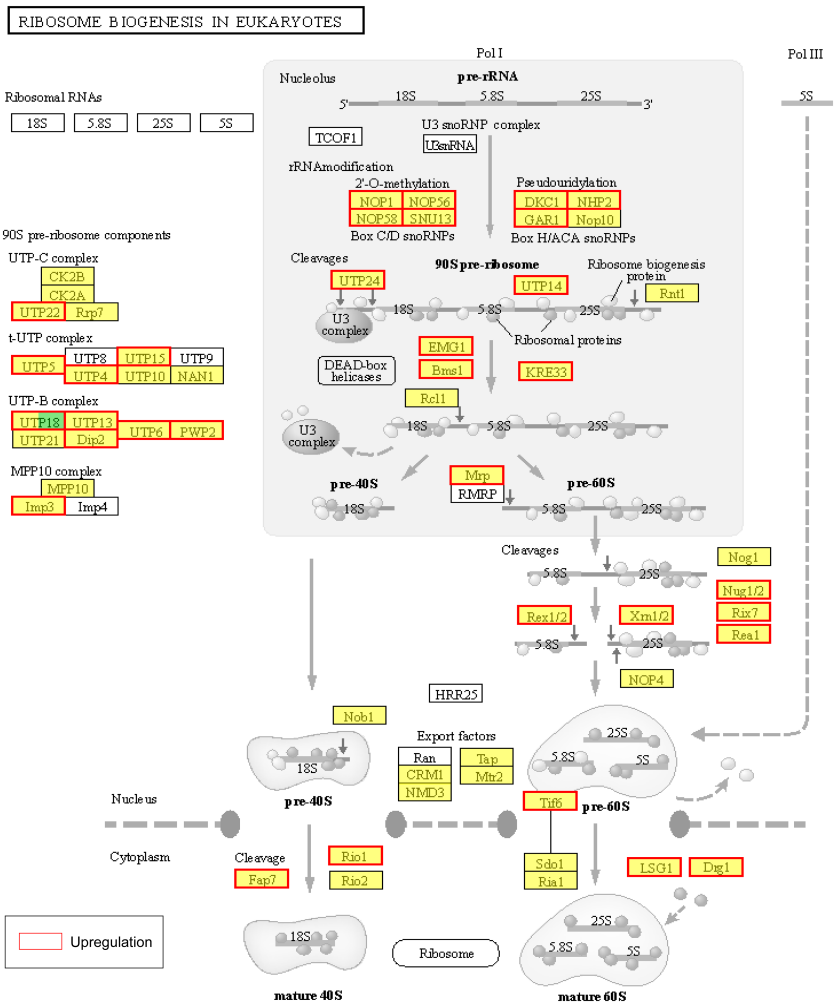

FIGURE 8
Changes of ribosome biogenesis during LO vs RO.

metabolism and cell molecular signal. Zhou et al. (2022) showed that the gastrointestinal microbiome could affect the resistance of *Cynoglossus semilaevis* by regulating host metabolism and signaling pathways. Additionally, a previous study on mammals showed a higher abundance of intestinal Bacteroidota and Firmicutes in hypoxia, which suggested that intestinal bacteria may be involved in host energy metabolism and facilitate organismal adaptation to hypoxic environments (Foley et al., 2016).

On the transcriptome level, compared with the NO group, KEGG enrichment analysis revealed that DEGs of the LO and RO groups were mainly annotated to pathways including the Steroid synthesis, Fatty acid synthesis, and Ribosome biogenesis in eukaryotes pathways, and they were also annotated to the PPAR signaling pathway, PI3K-Akt signaling pathway, and ECM-receptor interaction pathway. Compared with hypoxia, many URGs were enriched in the Ribosome biogenesis in eukaryotes pathway (Figure 8) and the Proteasome pathway (Figure 9) in the RO group. In eukaryotic cells, the ubiquitin–proteasome system and autophagy–lysosome system are two major protein degradation pathways; the proteasome removes excess damaged proteins during proteolytic activity (Nath and Shadan, 2009). Ribosomes are actively involved in protein folding during mRNA translation (Banerjee and Sanyal, 2014). Moreover, KEGG of microbiota was enriched in Signaling molecules and interaction. This suggests that the recovery process may also be regulated by the microbiota. Taken together, these results indicate that the clearance of misfolded proteins and the folding of new proteins play important roles in the recovery of the yellowtail kingfish during reoxygenation. In summary, the gastrointestinal microbiota and DEGs were all annotated to pathways associated with metabolism, cellular and molecular signaling, and protein repairment and synthesis; they may have synergetic function during the physiological adaptation changes of the yellowtail kingfish under hypoxia and reoxygenation, and the detailed mechanisms and pathways should be clarified in the future.

4.3 Changes in Steroid synthesis, PPAR signaling, and fatty acid synthesis pathways in response to hypoxia and reoxygenation

Unlike terrestrial animals that predominantly utilize carbohydrate, fish primarily use lipids and proteins as sources of

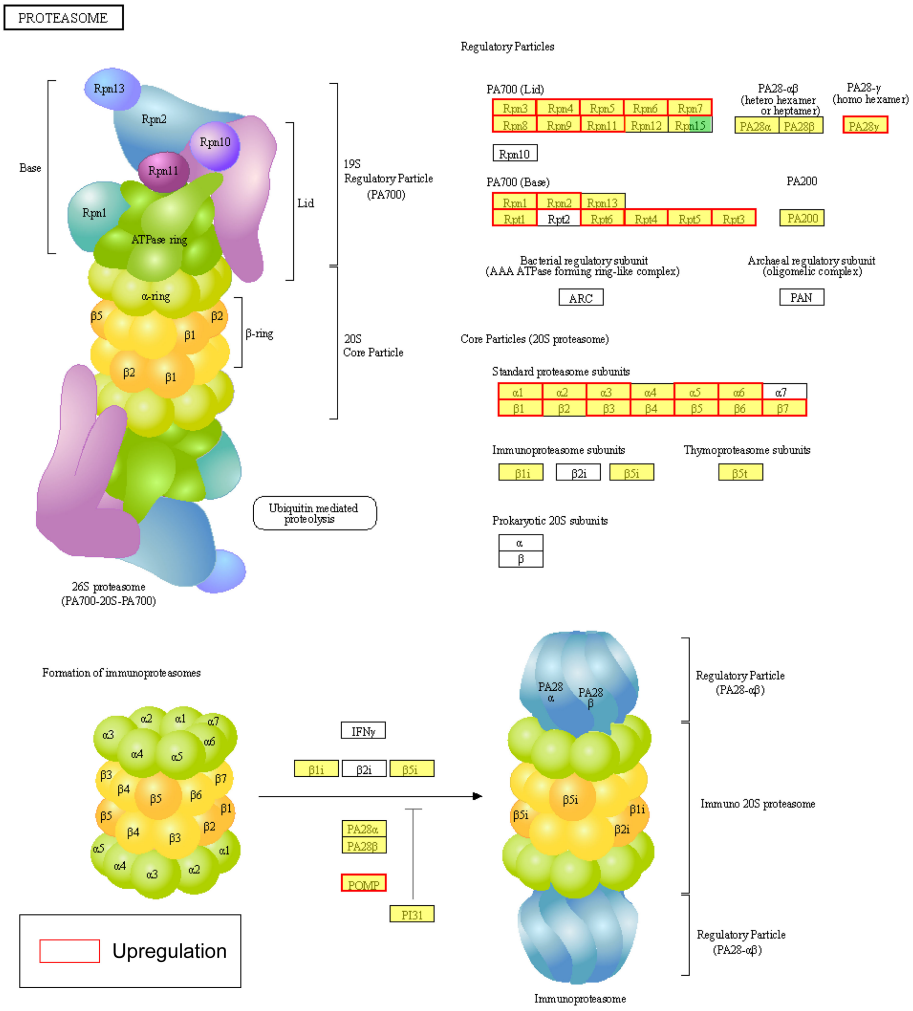

FIGURE 9
Changes of proteasome during LO vs RO.

energy because of their extremely poor ability to utilize carbohydrates (Zhao et al., 2022). It has been shown that the most critical aspects of the adaptation strategy of fish exposed to prolonged hypoxic levels is the adjustment of energy metabolism (Krumschnabel et al., 2000; Xiao, 2015). A recent study discovered that prolonged hypoxia significantly regulated the fatty acid metabolic pathway in zebrafish (*Danio rerio*) liver (Song et al., 2022). In addition, hypoxia inhibits the production of acetyl coenzyme A, which is required for fatty acid oxidation (Fuhrmann et al., 2019). We discovered very comparable outcomes in this study; the DEGs from LO and RO groups were mainly annotated to metabolic processes, and the Steroid biosynthesis and PPAR signaling pathways were significantly enriched (Figure 10).

In the Steroid biosynthesis pathway, genes including farnesyl diphosphate farnesyltransferase 1 (*FDFT1*), 24-dehydrocholesterol reductase (*DHCR24*), and sterol-C5 desaturase (*SC5DL*) were upregulated (Figure 10). *FDFT1* is a key gene participating in cholesterol synthesis (Dong et al., 2018), and these significantly upregulated genes may lead to the increase of cholesterol level. By assembling triglycerides and carrier proteins, cholesterol creates very low-density lipoprotein (VLPL) (Yoon et al., 2016), which subsequently enters the PPAR signaling pathway; it is then transported into the nucleus *via* fatty acid transport protein (*FATP*) and fatty acid-binding protein (*FABP*), and is mediated by different transcription factors in ligands, such as liver, skeletal muscle, and adipocytes regulating lipid differentiation and lipid metabolism (Poulsen et al., 2012). In addition, nuclear peroxisome proliferator-activated receptor α (*PPARα*) and stearoyl coenzyme A dehydrogenase-1 (*SCD-1*) regulate the genes involved in lipid metabolism in the liver and skeletal muscle. Another nuclear transcription factor, peroxisome proliferator-activated receptor γ (*PPARγ*), is activated by ligands and binds to retinoid X receptor to form a dimer whose binding site is in the promoter region of the adipocyte fatty acid-binding protein 4 (*FABP4*) gene (Gunnell et al., 2005). Additionally, angiopoietin-like protein 4 (*ANGPTL4*) was involved in adipocyte differentiation, and aquaporin 7 (*AQP7*) and phosphoenolpyruvate carboxykinase (*PEPCK*) were involved in

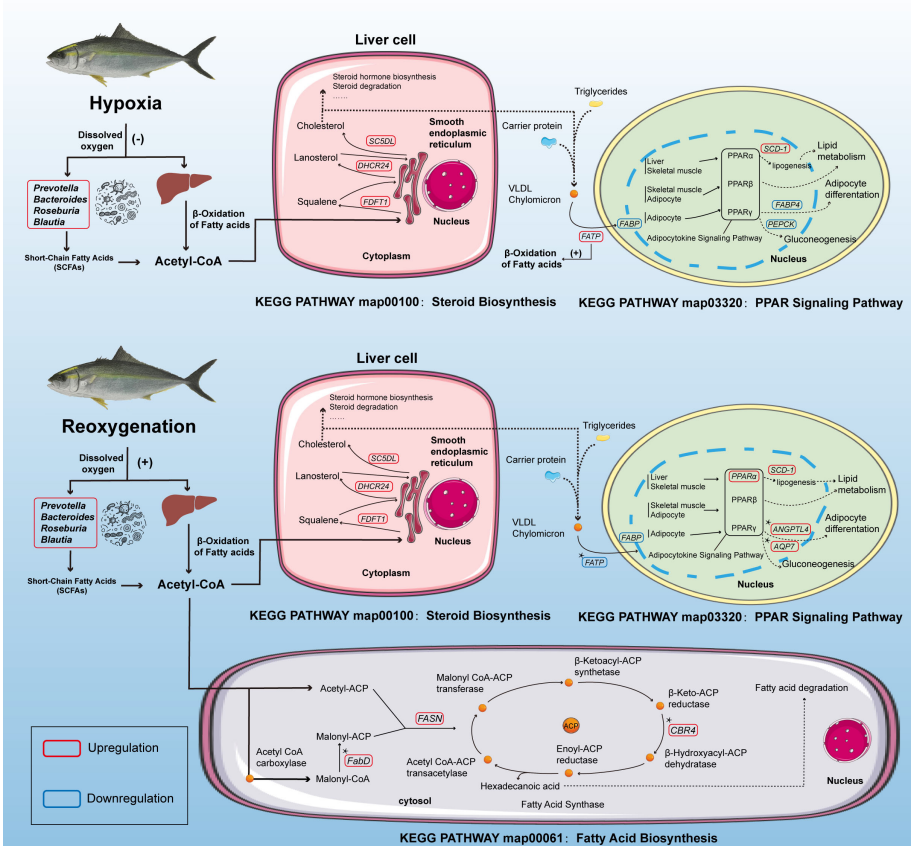

FIGURE 10
Changes in lipid metabolism in yellowtail kingfish under normoxia vs hypoxia and normoxia vs reoxygenation. * Indicates genes significantly regulated in hypoxia vs reoxygenation.

gluconeogenesis (Skowronski et al., 2007; Zhao et al., 2021). *PEPCK*, as a key rate-limiting enzyme of gluconeogenesis, is one of the indicators of changes in resistance of the organism (Yang et al., 2009; Yang et al., 2021).

In this study, the *FATP* gene was significantly upregulated, which indicated enhanced transportation ability of free fatty acids under hypoxia. The *FABP4* gene was significantly downregulated and the *SCD-1* gene was significantly upregulated, which indicated enhanced lipogenesis and weakened adipocyte differentiation (Singh et al., 2015). This metabolic pattern of reduced lipid deposition and increased lipid decomposition may be a highly efficient adaptive strategy of yellowtail kingfish to hypoxia. During reoxygenation, *PPARα*, *SCD-1*, *ANGPTL4*, and *AQP7* genes were significantly upregulated; these findings indicated that lipid accumulation and energy output were improved, which would facilitate the recovery of yellowtail kingfish from unbalanced energy homeostasis. In addition, an increasing number of studies have suggested that intestinal microbiota are involved in the regulation of host lipid metabolism (Velagapudi et al., 2010; Mestdagh et al., 2012; Allin et al., 2015; Sheng et al., 2018; Zhou et al., 2022). Camp et al. (2012) reported that colonization of intestinal microbiota affected the expression of the *ANGPTL4*, which is responsible for lipase regulation, using the sterile zebrafish model. The *ANGPTL4* gene in the PPAR signaling pathway was significantly upregulated in the RO group; this may have been modulated by the microbiota.

In the fatty acid synthesis pathway, genes such as fatty acid synthase (*FASN*) and monoacyl-CoA: ACP transacylase (*FabD*) genes were significantly upregulated in yellowtail kingfish (Figure 10). Recent studies have confirmed the involvement of the *FASN* gene in the deposition and composition of fat in cattle (*Bos grunniens*) muscle (Chu et al., 2015). In another study, a significant positive correlation was found between *FASN* expression and muscle fat content (Chen et al., 2004). This indicated that fatty acid synthesis is activated, which may boost the ability to synthesize fatty acids to enhance lipid metabolism; this allows the yellowtail kingfish to cope with the hypoxic stress. From the perspective of host gastrointestinal microbiota, the changes of lipid metabolism-related pathways may be regulated by part of the microbiota.

A previous study showed that *Prevotella* and *Bacteroides* in the gastrointestinal tract could produce SCFA (Chambers et al., 2015). *Prevotella* produce propionic acid through metabolism of oligofructose and arabinoxylan (Ley, 2016), and *Bacteroides* produce SCFA such as acetate and succinate through anaerobic respiration (Zafar and Saier, 2021). *Blautia* produces its main metabolite, acetic acid, by fermenting glucose in the host

gastrointestinal tract (Liu et al., 2021; Yang et al., 2021). Acetic acid is considered a precursor involved in the production of cholesterol and fatty acids, and propionic acid is mainly involved in gluconeogenesis in the liver and intestine (Delzenne and Williams, 2002; De Vadder et al., 2014). It is known that *Prevotella*, *Bacteroides*, *Roseburia*, and *Blautia* are anaerobic bacteria, and this is the main reason that their abundance increased in the gastrointestinal tract in the LO group. The increased relative abundance of these microbes also possibly resulted in the production of metabolites, such as acetic acid and propionic acid. Interestingly, we discovered that the relative abundances of *Prevotella* and *Bacteroides* in Bacteroidota, and *Roseburia* and *Blautia* in Firmicutes increased in the LO group and remained the same level in the RO group. Thus, our results suggested that the changes in relative abundances of *Prevotella*, *Bacteroides*, *Roseburia*, and *Blautia* in gastrointestinal microbiota may be mainly involved in the adaptation to hypoxic stress through SCFA metabolism in the yellowtail kingfish.

5 Conclusion

In the present study, we clarified the physiological responses of tolerance and adaptation to hypoxia and reoxygenation in a pelagic fish, the yellowtail kingfish. The gill structure change and recovery exhibited histological changes in response to hypoxia and reoxygenation. The relative abundance of microbiota producing SCFA, including *Prevotella*, *Bacteroides*, *Roseburia*, and *Blautia*, in the gastrointestinal tract were observed under both hypoxic and reoxygenation conditions. Furthermore, the DEGs were mainly enriched in pathways related to lipid metabolism, including Steroid biosynthesis and PPAR signaling pathways in the LO group and Steroid biosynthesis, Fatty acid biosynthesis, and PPAR signaling pathways in the RO group. KEGG analysis revealed that the gastrointestinal microbiota and DEGs were all annotated to pathways associated with metabolism, cellular and molecular signaling, and protein repairment and synthesis; they may have synergetic function during the physiological adaptation changes of the yellowtail kingfish under hypoxia and reoxygenation. The present results would be helpful to establish practical regulation technology for hypoxic stress adaptation in aquaculture of yellowtail kingfish.

Data availability statement

The datasets presented in this study can be found in online repositories. The names of the repository/repositories and accession number(s) can be found below: https://ngdc.cncb.ac.cn/gsa, GSA: CRA008447.

Ethics statement

The animal study was reviewed and approved by The Institutional Animal Care and Use Committee of Yellow Sea Fisheries Research Institute, Chinese Academy of Fishery Sciences.

Author contributions

Conceptualization, YX and HZ; methodology, YX and HZ; validation, YX, YJ, and HZ; formal analysis, HZ and YJ; investigation, HZ, AC, and YX; data curation, HZ, AC, YF, ZJ, and BW; writing—original draft preparation, HZ; writing—review and editing, HZ and YX; supervision, YX; funding acquisition, YX. All authors contributed to the article and approved the submitted version.

Funding

This research was funded by the National Key R&D Program of China (2022YFD2401102; 2019YFD0900901), the Central Public-interest Scientific Institution Basal Research Fund, CAFS (2020TD47), and the China Agriculture Research System of MOF and MARA (CARS-47).

Conflict of interest

The authors declare that the research was conducted in the absence of any commercial or financial relationships that could be construed as a potential conflict of interest.

Publisher's note

All claims expressed in this article are solely those of the authors and do not necessarily represent those of their affiliated organizations, or those of the publisher, the editors and the reviewers. Any product that may be evaluated in this article, or claim that may be made by its manufacturer, is not guaranteed or endorsed by the publisher.

Supplementary material

The Supplementary Material for this article can be found online at: https://www.frontiersin.org/articles/10.3389/fmars.2023.1121866/full#supplementary-material

References

Allin, K. H., Nielsen, T., and Pedersen, O. (2015). Mechanisms in endocrinology: Gut microbiota in patients with type 2 diabetes mellitus. *Eur. J. Endocrinol.* 172 (4), R167–R177. doi: 10.1530/EJE-14-0874

Banerjee, D., and Sanyal, S. (2014). Protein folding activity of the ribosome (PFAR) – a target for antiprion compounds. *Viruses* 6 (10), 3907–3924. doi: 10.3390/v6103907

Camp, J. G., Jazwa, A. L., Trent, C. M., and Rawls, J. F. (2012). Intronic cis-regulatory modules mediate tissue-specific and microbial control of angptl4/fiaf transcription. *PloS Genet.* 8 (3), e1002585. doi: 10.1371/journal.pgen.1002585

Caporaso, J. G., Kuczynski, J., Stombaugh, J., Bittinger, K., Bushman, F. D., Costello, E. K., et al. (2010). QIIME allows analysis of high-throughput community sequencing data. *Nat. Methods* 7 (5), 335–336. doi: 10.1038/nmeth.f.303

Chambers, E. S., Morrison, D. J., and Frost, G. (2015). Control of appetite and energy intake by SCFA: What are the potential underlying mechanisms? *Proc. Nutr. Soc.* 74 (3), 328–336. doi: 10.1017/S0029665114001657

Chen, S., Wang, P., Ou, Y., Li, J., Wen, J., Wang, W., et al. (2017). Acute and chronic hypoxia effect on gills of golden pompano (*Trachinotus ovatus*). *South China Fisheries Sci.* 13 (1), 124–130. doi: 10.3969/j.issn.2095-0780.2017.01.016

Chen, J., Yang, X. J., Tong, H., and Zhao, R. Q. (2004). Expressions of fas and hsl mrna in longissimus dorsi muscle and their relation to intramuscular fat contents in pig. *J. Agric. Biotechnol.* 12, 422–426. doi: 10.3969/j.issn.1674-7968.2004.04.014

Chen, S., Zhou, Y., Chen, Y., and Gu, J. (2018). Fastp: An ultra-fast all-in-one FASTQ preprocessor. *Bioinf. (Oxford England)* 34 (17), i884–i890. doi: 10.1093/bioinformatics/bty560

Chu, M., Wu, X. Y., Guo, X., Pei, J., Jiao, F., Fang, H. T., et al. (2015). Association between single-nucleotide polymorphisms of fatty acid synthase gene and meat quality traits in datong yak (*Bos grunniens*). *Genet. Mol. research: GMR* 14 (1), 2617–2625. doi: 10.4238/2015.March.30.21

Delzenne, N. M., and Williams, C. M. (2002). Prebiotics and lipid metabolism. *Curr. Opin. lipidology* 13 (1), 61–67. doi: 10.1097/00041433-200202000-00009

De Vadder, F., Kovatcheva-Datchary, P., Goncalves, D., Vinera, J., Zitoun, C., Duchampt, A., et al. (2014). Microbiota-generated metabolites promote metabolic benefits *via* gut-brain neural circuits. *Cell* 156 (1-2), 84–96. doi: 10.1016/j.cell.2013.12.016

de Vos, W. M., Tilg, H., Van Hul, M., and Cani, P. D. (2022). Gut microbiome and health: Mechanistic insights. *Gut* 71 (5), 1020–1032. doi: 10.1136/gutjnl-2021-326789

Ding, J., Liu, C., Luo, S., Zhang, Y., Gao, X., Wu, X., et al. (2020). Transcriptome and physiology analysis identify key metabolic changes in the liver of the large yellow croaker (*Larimichthys crocea*) in response to acute hypoxia. *Ecotoxicology Environ. Saf.* 189, 109957. doi: 10.1016/j.ecoenv.2019.109957

Dong, X., Shan, X., Fang, X., Gao, Y., Jiang, P., and Zhao, Z. (2018). Construction of overexpression shrna vectors of fdft1 gene and its verification in bovine fetal fibroblasts. *Chin. J. Veterinary Science.* 05), 1045–1050. doi: 10.16303/j.cnki.1005-4545.2018.05.35

Dunwoodie, S. L. (2009). The role of hypoxia in development of the mammalian embryo. *Dev. Cell* 17 (6), 755–773. doi: 10.1016/j.devcel.2009.11.008

Evans, D. H., Piermarini, P. M., and Choe, K. (2005). The multifunctional fish gill: Dominant site of gas exchange, osmoregulation, acid-base regulation, and excretion of nitrogenous waste. *Physiol. Rev.* 85, 97–177. doi: 10.1152/physrev.00050.2003

Foley, M. H., Cockburn, D. W., and Koropatkin, N. M. (2016). The sus operon: A model system for starch uptake by the human gut bacteroidetes. *Cell. Mol. Life sciences: CMLS* 73 (14), 2603–2617. doi: 10.1007/s00018-016-2242-x

Fuhrmann, D. C., Olesch, C., Kurrle, N., Schnütgen, F., Zukunft, S., Fleming, I., et al. (2019). Chronic hypoxia enhances β-Oxidation-Dependent electron transport *via* electron transferring flavoproteins. *Cells* 8 (2), 172. doi: 10.3390/cells8020172

Gunnell, D., Miller, L. L., Rogers, I., Holly, J. M.ALSPAC Study Team (2005). Association of insulin-like growth factor I and insulin-like growth factor-binding protein-3 with intelligence quotient among 8- to 9-year-old children in the Avon longitudinal study of parents and children. *Pediatrics* 116 (5), e681–e686. doi: 10.1542/peds.2004-2390

Helly, J. J., and Levin, L. A. (2004). Global distribution of naturally occurring marine hypoxia on continental margins. *Deep Sea Res. Part I Oceanographic Res. Papers* 51 (9), 1159–1168. doi: 10.1016/j.dsr.2004.03.009

Jiang, Y., Yu, C., Xu, Y., Liu, X., Cui, A., Wang, B., et al. (2022). Potential role of gastrointestinal microbiota in growth regulation of yellowtail kingfish *Seriola lalandi* in different stocking densities. *Fishes* 7 (4), 154. doi: 10.3390/fishes7040154

Kroeker, K. J., Bell, L. E., Donham, E. M., Hoshijima, U., Lummis, S., Toy, J. A., et al. (2020). Ecological change in dynamic environments: Accounting for temporal environmental variability in studies of ocean change biology. *Global Change Biol.* 26 (1), 54–67. doi: 10.1111/gcb.14868

Krumschnabel, G., Schwarzbaum, P. J., Lisch, J., Biasi, C., and Wieser, W. (2000). Oxygen-dependent energetics of anoxia-tolerant and anoxia-intolerant hepatocytes. *J. Exp. Biol.* 203 (Pt 5), 951–959. doi: 10.1242/jeb.203.5.951

Ley, R. E. (2016). Gut microbiota in 2015: *Prevotella* in the gut: Choose carefully. *Nat. Rev. Gastroenterol. Hepatol.* 13 (2), 69–70. doi: 10.1038/nrgastro.2016.4

Li, B., and Dewey, C. N. (2011). RSEM: Accurate transcript quantification from RNA-seq data with or without a reference genome. *BMC Bioinf.* 12, 323. doi: 10.1186/1471-2105-12-323

Li, M., Xu, X., Liu, S., Fan, G., Zhou, Q., and Chen, S. (2022). The chromosome-level genome assembly of the Japanese yellowtail jack *Seriola aureovittata* provides insights into genome evolution and efficient oxygen transport. *Mol. Ecol. Resour* 22, 2701-2712. doi: 10.1111/1755-0998.13648

Li, H. M., Zhang, C. S., Han, X. R., and Shi, X. Y. (2015). Changes in concentrations of oxygen, dissolved nitrogen, phosphate, and silicate in the southern yellow sea1980–2012: sources and seaward gradients. *Estuar. Coast. Shelf Sci.* 163 (SEP.20PT.A), 44–55. doi: 10.1016/j.ecss.2014.12.013

Liu, X., Mao, B., Gu, J., Wu, J., Cui, S., Wang, G., et al. (2021). *Blautia*-a new functional genus with potential probiotic properties? *Gut Microbes* 13 (1), 1–21. doi: 10.1080/19490976.2021.1875796

Liu, X., Xu, Y., Li, R., LÜ, Y., Shi, B., Ning, J., et al. (2017). Analysis and evaluation of nutritional composition of the muscle of yellowtail kingfish (*Seriola aureovittata*). *Prog. Fishery Sci.* 38 (1), 128–135. doi: 10.11758/yykxjz.20160722001

Love, M. I., Huber, W., and Anders, S. (2014). Moderated estimation of fold change and dispersion for RNA-seq data with DESeq2. *Genome Biol.* 15 (12), 550. doi: 10.1186/s13059-014-0550-8

Ma, S., Shu, X., and Wang, W. X. (2022). Responses of two marine fish to organically complexed zn: Insights from microbial community and liver transcriptomics. *Sci. total Environ.* 835, 155457. doi: 10.1016/j.scitotenv.2022.155457

Magoč, T., and Salzberg, S. L. (2011). FLASH: Fast length adjustment of short reads to improve genome assemblies. *Bioinf. (Oxford England)* 27 (21), 2957–2963. doi: 10.1093/bioinformatics/btr507

Mestdagh, R., Dumas, M. E., Rezzi, S., Kochhar, S., Holmes, E., Claus, S. P., et al. (2012). Gut microbiota modulate the metabolism of brown adipose tissue in mice. *J. Proteome Res.* 11 (2), 620–630. doi: 10.1021/pr200938v

Moreira, M., Schrama, D., Soares, F., Wulff, T., Pousão-Ferreira, P., and Rodrigues, P. (2017). Physiological responses of reared sea bream (*Sparus aurata linnaeus*1758) to an amyloodinium ocellatum outbreak. *J. fish Dis.* 40 (11), 1545–1560. doi: 10.1111/jfd.12623

Nath, D., and Shadan, S. (2009). The ubiquitin system. *Nature* 458, 421–421. doi: 10.1038/458421a

Pawlus, M. R., and Hu, C. J. (2013). Enhanceosomes as integrators of hypoxia inducible factor (HIF) and other transcription factors in the hypoxic transcriptional response. *Cell. signalling* 25 (9), 1895–1903. doi: 10.1016/j.cellsig.2013.05.018

Petersen, L. H., and Gamperl, A. K. (2010). Effect of acute and chronic hypoxia on the swimming performance, metabolic capacity and cardiac function of Atlantic cod (*Gadus morhua*). *J. Exp. Biol.* 213 (5), 808–819. doi: 10.1242/jeb.033746

Pichavant, K., Person-Le-Ruyet, J., Bayon, N. L., Sévère, A., and Boeuf, G. (2000). Effects of hypoxia on growth and metabolism of juvenile turbot. *Aquaculture* 188 (1), 103–114. doi: 10.1016/S0044-8486(00)00316-1

Poulsen, L., Siersbæk, M., and Mandrup, S. (2012). PPARs: Fatty acid sensors controlling metabolism. *Semin. Cell Dev. Biol.* 23 (6), 631–639. doi: 10.1016/j.semcdb.2012.01.003

Ramírez, C., Rojas, R., and Romero, J. (2020). Partial evaluation of autochthonous probiotic potential of the gut microbiota of *Seriola lalandi*. *Probiotics antimicrobial Proteins* 12 (2), 672–682. doi: 10.1007/s12602-019-09550-9

San, L., Liu, B., Liu, B., Guo, H., Guo, L., Zhang, N., et al. (2021). Transcriptome analysis of gills provides insights into translation changes under hypoxic stress and reoxygenation in golden pompano, *Trachinotus ovatus* (Linnaeus 1758). *Front. Mar. Sci.* 8. doi: 10.3389/fmars.2021.76362

Sheng, Y., Ren, H., Limbu, S. M., Sun, Y., Qiao, F., Zhai, W., et al. (2018). The presence or absence of intestinal microbiota affects lipid deposition and related genes expression in zebrafish (*Danio rerio*). *Front. Microbiol.* 9. doi: 10.3389/fmicb.2018.01124

Shi, Q. (2016). Mechanism and spatio-temporal mode on the seasonal cycle of dissolved oxygen content fields in the yellow Sea. *J. Appl. Oceanography* 35 (01), 1–14. doi: 10.3969/J.ISSN.2095-4972.2016.01.001

Singh, V., Chassaing, B., Zhang, L., San Yeoh, B., Xiao, X., Kumar, M., et al. (2015). Microbiota-dependent hepatic lipogenesis mediated by stearoyl CoA desaturase 1 (SCD1) promotes metabolic syndrome in TLR5-deficient mice. *Cell Metab.* 22 (6), 983–996. doi: 10.1016/j.cmet.2015.09.028

Skowronski, M. T., Lebeck, J., Rojek, A., Praetorius, J., Füchtbauer, E. M., Frøkiaer, J., et al. (2007). AQP7 is localized in capillaries of adipose tissue, cardiac and striated muscle: Implications in glycerol metabolism. *American journal of physiology. Renal Physiol.* 292 (3), F956–F965. doi: 10.1152/ajprenal.00314.2006

Sollid, J., De Angelis, P., Gundersen, K., and Nilsson, G. E. (2003). Hypoxia induces adaptive and reversible gross morphological changes in crucian carp gills. *J. Exp. Biol.* 206 (Pt 20), 3667–3673. doi: 10.1242/jeb.00594

Song, R., Hu, R., Li, G., Zhang, Z., and Xu, Q. (2022). Research on effect of hypoxia stress on liver tissue of zebrafish (*Danio rerio*) based on transcriptomics technology. *South China Fisheries Sci.* doi: 10.12131/20220038

Sun, J., Liu, Y., Li, Y., Song, F., Wen, X., and Luo, J. (2021). Golden pompano (*Trachinotus blochii*) adapts to acute hypoxic stress by altering the preferred mode of energy metabolism. *Aquaculture* 542, 736842. doi: 10.1016/j.aquaculture.2021.736842

Ursell, L. K., Haiser, H. J., Van Treuren, W., Garg, N., Reddivari, L., Vanamala, J., et al. (2014). The intestinal metabolome: An intersection between microbiota and host. *Gastroenterology* 146 (6), 1470–1476. doi: 10.1053/j.gastro.2014.03.001

Vedor, M., Queiroz, N., Mucientes, G., Couto, A., Costa, I. D., Santos, A. D., et al. (2021). Climate-driven deoxygenation elevates fishing vulnerability for the ocean's widest ranging shark. *eLife* 10, e62508. doi: 10.7554/eLife.62508

Velagapudi, V. R., Hezaveh, R., Reigstad, C. S., Gopalacharyulu, P., Yetukuri, L., Islam, S., et al. (2010). The gut microbiota modulates host energy and lipid metabolism in mice. *J. Lipid Res.* 51 (5), 1101–1112. doi: 10.1194/jlr.M002774

Wang, W. Z., Huang, J. S., and Zhang, J. D. (2021). Effects of hypoxia stress on the intestinal microflora of juvenile of cobia (*Rachycentron canadum*). *Aquaculture 536* 736419, . doi: 10.1016/j.aquaculture.2021.736419

Wu, C. B., Liu, Z. Y., Li, F. G., Chen, J., Jiang, X. Y., and Zou, S. M. (2017). Gill remodeling in response to hypoxia and temperature occurs in the hypoxia sensitive blunt snout bream (*Megalobrama amblycephala*). *Aquaculture* 479, 479–486. doi: 10.1016/j.aquaculture.2017.06.020

Xiao, W. (2015). The hypoxia signaling pathway and hypoxic adaptation in fishes. *Sci. China. Life Sci.* 58 (2), 148–155. doi: 10.1007/s11427-015-4801-z

Xie, C., Mao, X., Huang, J., Ding, Y., Wu, J., Dong, S., et al. (2011). KOBAS 2.0: A web server for annotation and identification of enriched pathways and diseases. *Nucleic Acids Res.* 39 (Web Server issue), W316–W322. doi: 10.1093/nar/gkr483

Xu, Y., Zhang, Z., Liu, X., Wang, B., Shi, B., Liu, Y., et al. (2019). Early growth and development characteristics of *Seriola lalandi*. *J. Fishery Sci. China* 26 (1), 172–182. doi: 10.3724/SP.J.1118.2019.18094

Yang, J., Kalhan, S. C., and Hanson, R. W. (2009). What is the metabolic role of phosphoenolpyruvate carboxykinase? *J. Biol. Chem.* 284 (40), 27025–27029. doi: 10.1074/jbc.R109.040543

Yang, X. L., Wang, G., Xie, J. Y., Li, H., Chen, S. X., Liu, W., et al. (2021). The intestinal microbiome primes host innate immunity against enteric virus systemic infection through type I interferon. *mBio* 12 (3), e00366–e00321. doi: 10.1128/mBio.00366-21

Yoon, H., Flores, L. F., and Kim, J. (2016). MicroRNAs in brain cholesterol metabolism and their implications for alzheimer's disease. *Biochim. Biophys. Acta* 1861 (12 Pt B), 2139–2147. doi: 10.1016/j.bbalip.2016.04.020

Zafar, H., and Saier, M. H.Jr (2021). Gut bacteroides species in health and disease. *Gut Microbes* 13 (1), 1–20. doi: 10.1080/19490976.2020.1848158

Zhao, X., Huang, H., Ding, X., Yang, Z., Hou, Y., and Wang, H. (2021). Angiopoietin-like protein 4 regulates breast muscle lipid metabolism in broilers. *Poultry Sci.* 100 (7), 101159. doi: 10.1016/j.psj.2021.101159

Zhao, L., Wang, D., Liao, Z., Bi, Q., Ma, Q., Wei, Y., et al. (2022). Tissue distribution and nutritional regulation of fatty acid transport protein in *Scophthalmus maximus* and *Takifugu rubripes*. *Chin. J. Anim. Nutr.* 34 (10), 6620–6633. doi: 10.3969/j.issn.1006-267x.2022.10.055

Zhou, Q., Zhu, X., Li, Y., Yang, P., Wang, S., Ning, K., et al. (2022). Intestinal microbiome-mediated resistance against vibriosis for cynoglossus semilaevis. *Microbiome* 10 (1), 153. doi: 10.1186/s40168-022-01346-4